

Parametric Amplification of Spectrally Incoherent Signals

C. Dorrer

Laboratory for Laser Energetics, University of Rochester

Optical parametric amplifiers (OPA's) compare favorably with laser amplifiers in terms of spectral coverage and broadband operation. Their properties, and in particular the efficiency of the energy transfer between the pump and the signal, have been extensively studied for a spectrally coherent signal,^{1,2} but there are no complete studies of parametric amplification for spectrally incoherent pulses. These pulses are highly relevant to the mitigation of laser–plasma instabilities in high-energy laser–matter interactions.^{3–6} They are the basis for the fourth-generation laser for ultrabroadband experiments (FLUX) currently being built at LLE, where three stages of parametric amplifiers will amplify spectrally incoherent broadband signals. A framework supporting OPA simulations using normalized equations is developed and used to analyze OPA operation with a spectrally incoherent signal, in particular amplification performance and statistical properties of the amplified signal, showing the interplay between OPA properties and initial seeding conditions. These simulations are in agreement with an experimental demonstration of optical parametric amplification with various spectrally incoherent signals.⁷

A set of normalized equations is developed to describe the amplification of a spectrally incoherent signal with coherence time $\Delta\tau$ by a monochromatic pump at a constant intensity $I_{p,0}$. The three-wave nonlinear mixing equations in the absence of group-velocity dispersion² can be normalized into

$$\begin{aligned} \frac{\partial A_s}{\partial z} + \frac{1}{v_s} \frac{\partial A_s}{\partial t} &= -j \frac{\omega_s d_{\text{eff}}}{cn_s} A_i^* A_p \Rightarrow \frac{\partial a_s}{\partial Z} = -j a_i^* a_p, \\ \frac{\partial A_i}{\partial z} + \frac{1}{v_i} \frac{\partial A_i}{\partial t} &= -j \frac{\omega_i d_{\text{eff}}}{cn_i} A_s^* A_p \Rightarrow \frac{\partial a_i}{\partial Z} + \frac{\delta_i}{\Gamma} \frac{\partial a_i}{\partial \tau} = -j a_s^* a_p, \\ \frac{\partial A_p}{\partial z} + \frac{1}{v_p} \frac{\partial A_p}{\partial t} &= -j \frac{\omega_p d_{\text{eff}}}{cn_p} A_s A_i \Rightarrow \frac{\partial a_p}{\partial Z} + \frac{\delta_p}{\Gamma} \frac{\partial a_p}{\partial \tau} = -j a_s a_i. \end{aligned} \quad (1)$$

The fields of the pump A_p , signal A_s , and idler A_i , as a function of time t and longitudinal position z , are normalized according to $a_s = A_s \sqrt{\varepsilon_0 n_s c \omega_p / 2 I_{p,0} \omega_s}$, $a_i = A_i \sqrt{\varepsilon_0 n_i c \omega_p / 2 I_{p,0} \omega_i}$, and $a_p = A_p \sqrt{\varepsilon_0 n_p c / 2 I_{p,0}}$. The OPA is characterized by the temporal walk-off of the idler and pump relative to the signal, δ_i and δ_p , and the commonly used nonlinear coefficient $\Gamma = \sqrt{2 d_{\text{eff}}^2 \omega_1 \omega_2 I_{p,0} / c^3 \varepsilon_0 n_s n_i n_p}$ related to its small-signal gain.²

The quantities $\Phi_s = |a_s|^2 = I_s \omega_p / I_{p,0} \omega_s$, $\Phi_i = |a_i|^2 = I_i \omega_p / I_{p,0} \omega_i$, and $\Phi_p = |a_p|^2 = I_p / I_{p,0}$ are the ratios of the photon flux for the signal, idler, and pump, respectively, at a given time and position to the input-pump photon flux. For a monochromatic signal, the increase in Φ_s and Φ_i during amplification are equal and reach a limit value equal to 1 at full pump depletion (Manley–Rowe relations). The normalized equations allow for general simulations over the properties of the crystal and initial conditions (signal coherence time and input relative energy of the signal and pump), highlighting their impact on the amplification of a spectrally incoherent signal such as the one presented in Fig. 1, which has the expected negative exponential probability density function (pdf). Such a signal, with an initial average photon flux of 4×10^{-6} , leads to pump saturation in an OPA with a small-signal gain equal to 10^6 .

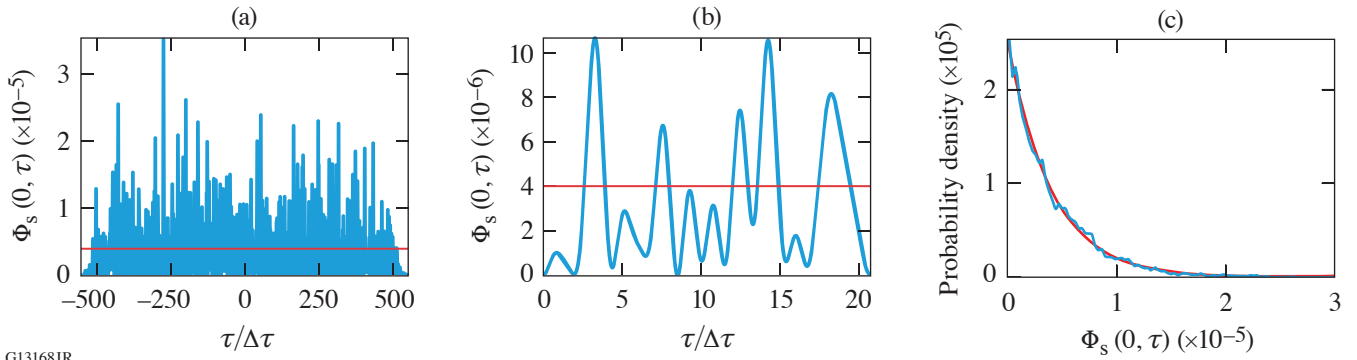


Figure 1 Photon flux ratio for the signal (blue curve) as a function of time normalized to the coherence time over (a) the entire pulse and (b) a time range corresponding to 20 coherence times, where the red line represents the time-averaged photon flux ratio $\Phi_{s,0} = 4 \times 10^{-6}$. (c) Probability density function of the input signal (blue curve) and negative exponential with the same average value (red curve).

An OPA with a small-signal gain equal to 10^6 and no significant idler-signal temporal walk-off (e.g., type-I phase matching close to spectral degeneracy, where the signal wavelength is approximately twice the pump wavelength) is first considered. In the undepleted-pump regime (low signal average flux, $\Phi_{s,0} = 4 \times 10^{-7}$), the amplified signal is proportional to the input signal and maintains a negative-exponential pdf [Fig. 2(a)]. With higher pump depletion [$\Phi_{s,0} = 1.26 \times 10^{-6}$, Fig. 2(b)], at low pump-signal temporal walk-off relative to the signal coherence time stationarity of the signal relative to the pump imposes $\Phi_s < 1$. In longer

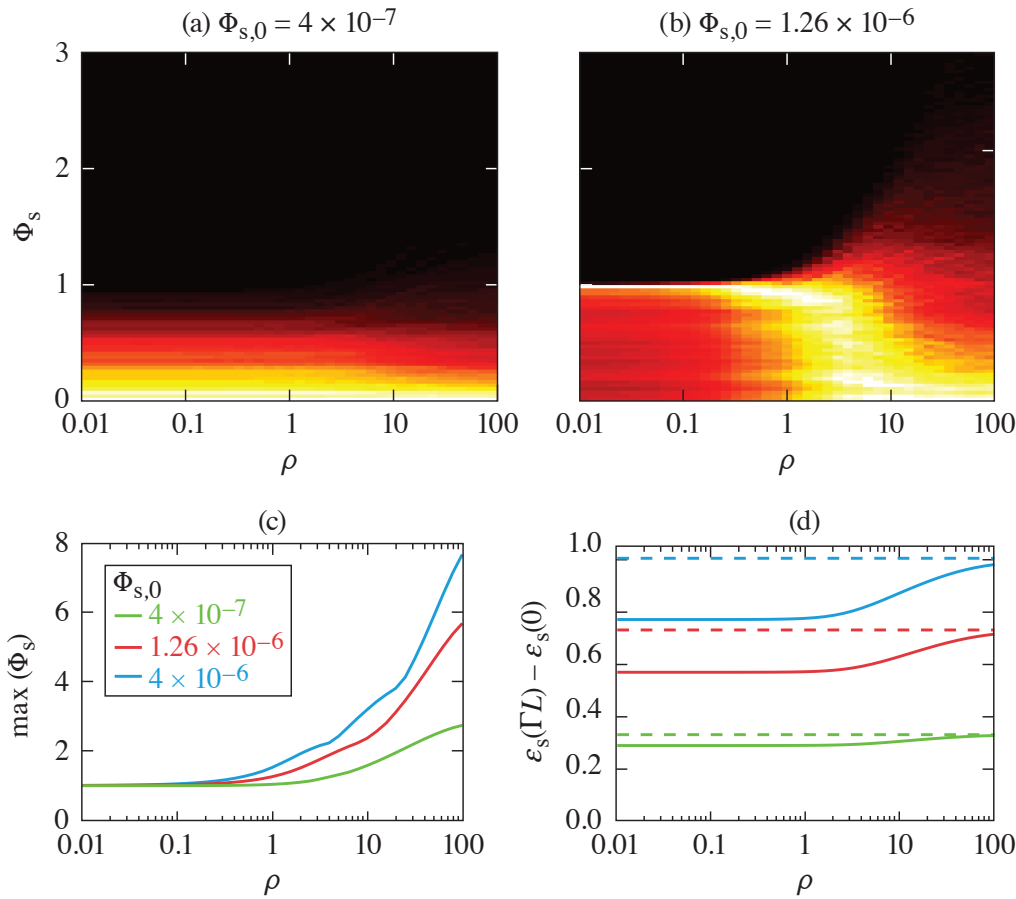


Figure 2 Probability density histograms of the amplified signal as a function of the pump-signal temporal walk-off normalized to the signal coherence time $\rho = \delta_p / \Delta\tau$ in (a) the undepleted-pump regime and (b) with some pump depletion. [(c),(d)] The highest values of the signal photon flux and energy increase as a function of ρ for three depletion conditions.

G13230JR

crystals ($\rho > 1$), however, the signal extracts energy from various temporal slices of the pump, allowing for Φ_s much larger than 1 at some particular times [Figs. 2(b) and 2(c)] and a slight increase in the extracted energy [Fig. 2(d)]. While the pdf is expected to be sharply peaked below 1 at small temporal walk-off, it follows a negative exponential function at large temporal walk-off.

A nonzero idler-signal temporal walk-off limits the amplification efficiency when the signal and idler are relatively shifted by a delay larger than the coherence time $\Delta\tau$, i.e., when $\delta_i L > \Delta\tau$, where L is the crystal length, as indicated by vertical dashed lines on Fig. 3(a) for $\delta_i = \delta_p/10$ and $\delta_i = \delta_p$. Considering that the signal bandwidth is inversely proportional to its coherence time, the energy decrease is fundamentally linked to the OPA phase mismatch, $\delta_i L/\Delta\tau$, as confirmed by the calculated relative bandwidth [Fig. 3(b)]. Spectrally incoherent signals offer an intuitive time-domain picture of the OPA phase mismatch, which is most often described in the spectral domain.

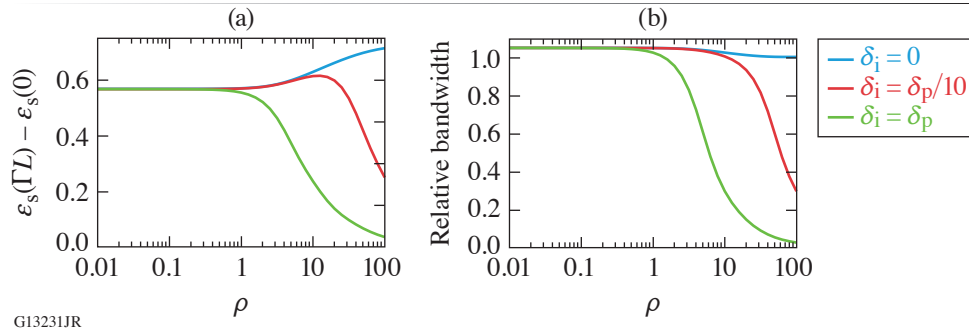


Figure 3

(a) Extracted energy as a function $\rho = \delta_p/\Delta\tau$ for three different ratios δ_i/δ_p . (b) Bandwidth of the amplified signal relative to the initial bandwidth.

Simulations performed with normalized equations are in excellent agreement with simulations that take into account the full dispersion properties of specific nonlinear crystals (BBO, LBO, DKDP). In particular, broadband operation is observed in type-I crystals at spectral degeneracy, while the idler-signal temporal walk-off limits the OPA efficiency when operating away from degeneracy or in type-II crystals.

This material is based upon work supported by the Department of Energy National Nuclear Security Administration under Award Number DE-NA0003856, the University of Rochester, and the New York State Energy Research and Development Authority.

1. R. A. Baumgartner and R. Byer, *IEEE J. Quantum Electron.* **15**, 432 (1979).
2. G. Cerullo and S. De Silvestri, *Rev. Sci. Instrum.* **74**, 1 (2003).
3. J. J. Thomson and J. I. Karush, *Phys. Fluids* **17**, 1608 (1974).
4. S. P. Obenschain, N. C. Luhmann, and P. T. Greiling, *Phys. Rev. Lett.* **36**, 1309 (1976).
5. J. P. Palastro *et al.*, *Phys. Plasmas* **25**, 123104 (2018).
6. R. K. Follett *et al.*, *Phys. Plasmas* **26**, 062111 (2019).
7. C. Dorrer, E. M. Hill, and J. D. Zuegel, *Opt. Express* **28**, 451 (2020).